03.1

# Mixing of gas jets of different molecular weights with a high-speed air flow when their dynamic head is changed

© A.S. Akinin, T.A. Korotaeva, A.V. Starov

Khristianovich Institute of Theoretical and Applied Mechanics, Siberian Branch, Russian Academy of Sciences, Novosibirsk, Russia
E-mail: starov@itam.nsc.ru

*Received May 25, 2023*
*Revised July 3, 2023*
*Accepted July 3, 2023*

The results of a computational and experimental study of the distributed transverse injection of hydrogen and methane jets into a high-speed flow are presented. The effect of jets on the flow structure in a rectangular channel of a variable cross section is determined when the dynamic head coefficient changes in the range 1.27-6. It is shown that the mixing efficiency increases with an increase in the dynamic head and, to a lesser extent, with an increase in the molecular weight of the injected gas.

**Keywords:**high-speed flow, injection, dynamic head, mixing.

DOI: 10.61011/TPL.2023.09.56701.19639

The introduction of gas jets with various inherent characteristics in the initial cross section of a channel leads to a considerable change in the structure of flow along the channel [1]. This alteration of the flow structure translates into qualitative changes in static parameters (temperature and pressure) and in the efficiency of mixing of injected gas and the primary flow. A considerable number of numerical and experimental studies focused on different injection arrangements have already been published [2]. Transverse (with respect to the flow) injection through nozzles in channels walls [3–5] is one of the most widely used and reliable configurations that ensure rapid mixing of gas with air and deep penetration of jets into high-speed flows. The penetration of jets depends on several parameters: shape of the nozzle outlet, number of injectors, chemical composition and molecular mass of injected gas, etc. [6]. Most studies are focused on the injection of jets of incombustible gases (air, nitrogen, helium, and argon [6–9]), hydrogen [6,9–11], and ethylene [4]. The differences in molecular mass translate into a spread of injection speeds, affecting the rate of growth of a shear layer and the efficiency of mixing [4,8]. The use of methane in power and transport plants has attracted increasing interest in recent years. At the same time, the number of studies on injection of methane [8] into a high-enthalpy flow still remains much lower than the corresponding number for other gases. It has been demonstrated that the ratio of momenta of a gas jet and a flow is one of the key parameters affecting the mixing efficiency [8–11]. Therefore, since methane is such a promising fuel material, it appears relevant to determine the characteristics of its mixing within a wide range of injection pressures. The interaction of jets from multiple injectors complicates further the flow pattern in a channel with walls confining these jets. A complex internal channel structure induces the formation of shock waves and expansion waves and their interaction with the boundary layer on walls, affecting the disintegration of injected gas jets [12]. Since a considerable number of studies [8,13] have been performed with the use of a plate in free flow and/or a single injected jet [9], additional research is needed.

The aim of the present study is to determine the influence of multijet transverse injection of gases of different molecular masses on the structure of a high-enthalpy flow in a channel. The mixing of hydrogen and methane (without chemical reactions) with a primary flow with Mach number $M = 2.83$ was examined under variation of their dynamic head.

Experiments were carried out in the attached pipeline regime with a discharge stagnation chamber of a hot-shot wind tunnel, where electric arc heating to high temperature and pressure levels was performed [14,15], used as a source of working gas. Nitrogen (total temperature: 1934 K; total pressure: 3.27 MPa; flow rate: 0.85 kg/s) was the working gas. Stagnation parameters were determined in the second stagnation chamber of the setup. The Mach number of the incoming flow was determined in the cross section in front of injection orifices. Gases were injected at an angle of 90° from the wall through eight sonic nozzles (four on top and four at the bottom) in front of a backward-facing step (two-fold expansion of the channel in the vertical plane). Dynamic head coefficient $J = (\rho U^2)_{jet}/(\rho U^2)_\infty$ of a jet ($\rho$ is density and $U$ is speed), which is the ratio of dynamic heads of a jet and an incoming flow ($\infty$), was varied within the range from 1.27 to 6 due by adjusting the total supply pressure of injected gas (from 1.76 to 8.33 MPa for hydrogen and from 1.83 to 8.88 MPa for methane at a total temperature of 300 K).

Three-dimensional numerical modeling was performed in ANSYS FLUENT. Reynolds-averaged steady-state Navier–Stokes equations were solved for the turbulent

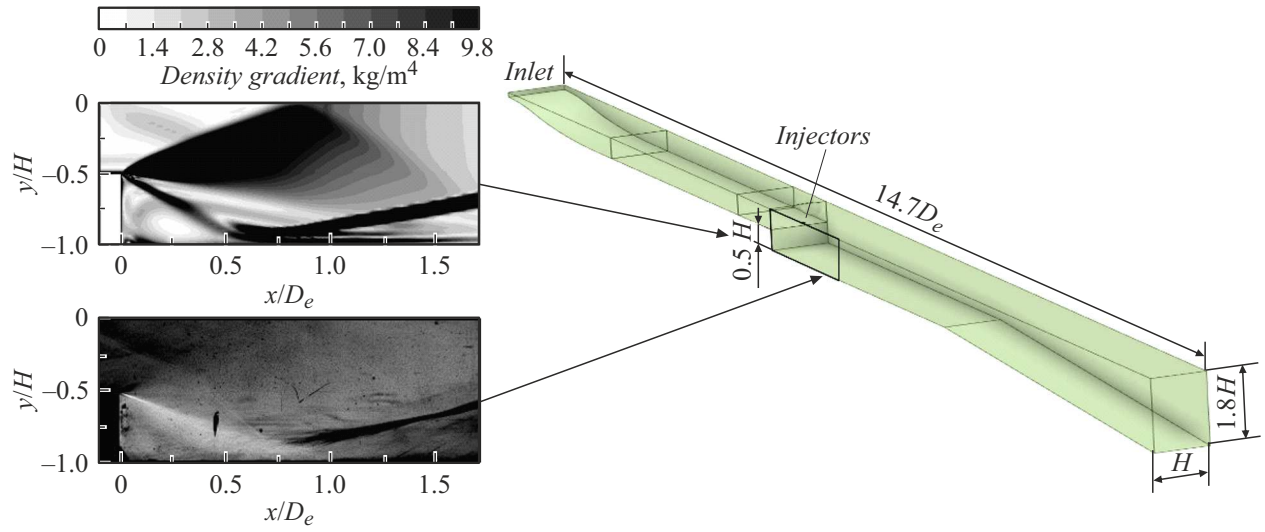


**Figure 1.** Diagram of the region of computation and schlieren image (bottom) of a section behind a backward-facing step in comparison with the flow pattern calculated for the case without gas injection.

multicomponent flow regime with the use of the $k-\omega$ SST turbulence model. The implicit AUSM second-order scheme was used to determine the flow parameters. Regular hexagonal meshes were generated by ANSYS ICEM CFD. Calculations were performed from the nozzle throat section. Since the channel is symmetric (Fig. 1), one quarter of it was considered. Mach number $M = 1$ and total head parameters determined experimentally were set at the inlet. The characteristic dimensions of the model channel are gauged in units of $D_e = 79.8$ mm, where $D_e = \sqrt{4A/\pi}$ is the equivalent channel diameter and $A$ is the channel cross section area in front of the injectors. The cross section remains constant within a stretch $3.82D_e$ in length located behind the backward-facing step. The relative length of the section expanding in the vertical plane is $x/D_e = 4.76$. Testing for convergence on computation meshes with $\sim (2, 4, 8) \cdot 10^6$ cells, we found that a $4 \cdot 10^6$ mesh is acceptable. The mesh was generated with refinement toward the wall in such a way that the values of wall function $y^+$ were on the order of unity. Stagnation pressure $P_0$, static pressure $p$, and stagnation temperature were set as the initial conditions at the left (inlet) boundary of the region of computation. The no-slip boundary condition was set at the channel walls with temperature $T_w = 300$ K, and symmetry conditions were specified at the front and upper boundaries of the region of computation. The conditions corresponding to that type of boundary were set at the outlet boundary of the region of computation. Ideal gas with constant thermal capacity and thermal conductivity was examined; its viscosity followed the Sutherland law.

The calculated density gradient field (Fig. 1) highlights the characteristic flow components: expansion fan at the step edge; mixing layer with a recirculation zone; reattachment shock. Combined with experimental data, a wide range of available calculated parameters provides an opportunity to analyze thoroughly the specific features of flow in given conditions.

A typical saw-tooth distribution of relative static pressure (normalized by the static pressure measured at a distance of 100 mm to injectors) with two peaks at 1.5 and 4.5 gauges is established at channel walls behind the step (Fig. 2, *a*). The pressure is maximized behind the reattachment shock within the stretch with a constant cross section. An expansion fan at the beginning of the expanding section reduces the static pressure, which reaches a local minimum close to the base pressure level behind the step. The second static pressure peak is seen behind the area of reattachment of a reflected shock. Its magnitude is approximately two times lower due to the accumulation of total pressure losses and to the acceleration of flow in the expanding channel (the mean Mach number is approximately 40% higher than the initial one at the inlet). The system of compression/expansion waves within the stretch with a constant cross section is presented in Fig. 2, *c*. It can be seen that shock waves are curved fairly strongly (with a greater angle at the flow core). The pattern is reversed after rereflection at the symmetry axis: the angle increases toward the channel walls (i.e., the angle of an individual element increases with increasing coordinate $x$ in every region of the shock wave system).

The injection of gas induces an upstream shift of the wave structure in the channel (Fig. 2). The shift magnitude increases with dynamic head coefficient $J$; notably, the first pressure maximum undergoes a somewhat smaller shift than the second maximum. At $J = 6$, the shift reaches a magnitude of $1-1.2$ gauges (relative to the no-injection case). It varies almost linearly with $J$ in the examined range. Experimental and calculated data agree qualitatively and quantitatively. Hydrogen jets produce flattened (broadened) pressure peaks. With coefficients $J$ being equal, methane jets induce a greater upstream shift

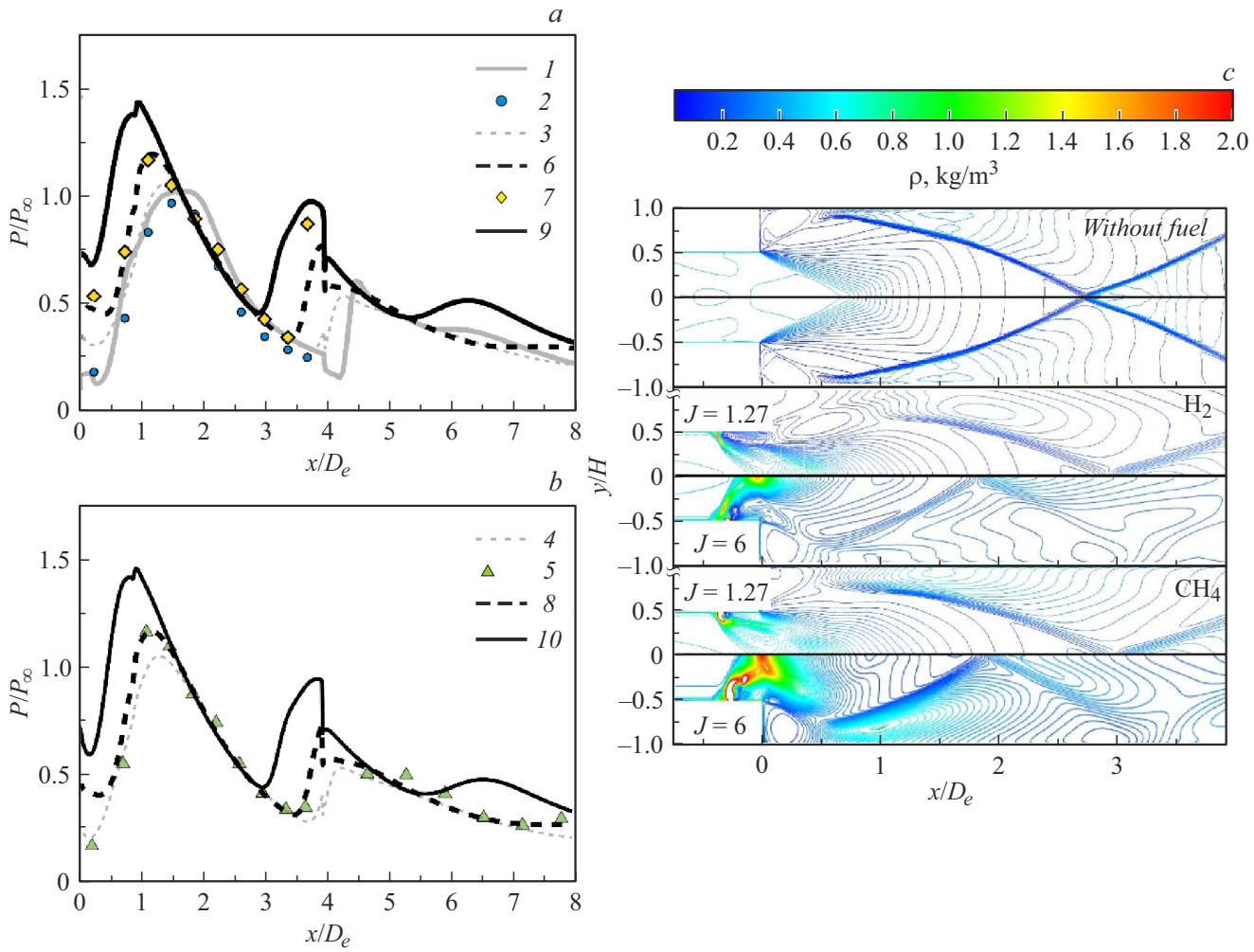


**Figure 2.** Distributions of relative static pressure along the channel for hydrogen ($a$) and methane ($b$) and calculated density fields ($c$) for various $J$. $J = 0$ ($1, 2$), 1.27 ($3–5$), 3 ($6–8$), and 6 ($9, 10$). Curves and symbols represent calculated and experimental data, respectively.

of the wave structure, but the magnitude of shift of maxima is insignificant compared to the width of pressure peaks. The qualitative flow patterns (Fig. 2, $c$) corresponding to hydrogen and methane injection differ more significantly. It is evident that the penetration of methane jets and their interaction with the primary flow produce a more complex flow pattern in the region of the backward-facing step and enhance the density difference in shock waves typical of the channel. This behavior may be attributed to the fact that methane has a higher molecular mass; consequently, the density of the primary flow needed to reach the same dynamic head coefficient of a jet increases.

Since total pressure losses accompany the flow in a channel with a varying cross section, the coefficients of total pressure loss over the channel length were determined as the ratio of the area-averaged total pressure in the outlet section to the pressure in the section in front of the injectors. In the case with no injection, the coefficient was 0.82. The coefficient decreases with increasing injected gas flow rate (rising $J$): at the maximum value of $J = 6$, it was just 0.51 for hydrogen and 0.44 for methane.

The results of numerical modeling provide an opportunity to determine the mixing efficiency based on the distribution of mass concentration of injected gases over the studied channel volume. Figure 3, $a$ presents the fields of mass fraction of methane in three longitudinal and seven transverse sections. It is evident that the concentration reaches its maximum directly at the gas injection orifices. The interaction of jets with the primary flow produces shock waves that, acting from opposite walls, shift the jets toward the channel wall behind the step. The flow turn behind the reattachment shock shifts the methane concentration maximum to the flow core (the central plane of the channel) and suppresses this maximum; notably, jets from individual sonic nozzles do not cross until reaching approximately the middle of the stretch with a constant cross section. The concentration at the flow core levels out in both longitudinal and transverse sections (with a reduction toward the channel walls) by the end of the stretch with a constant cross section. Within the final stretch, the concentration field becomes so uniform that individual jets are unidentifiable. The mass

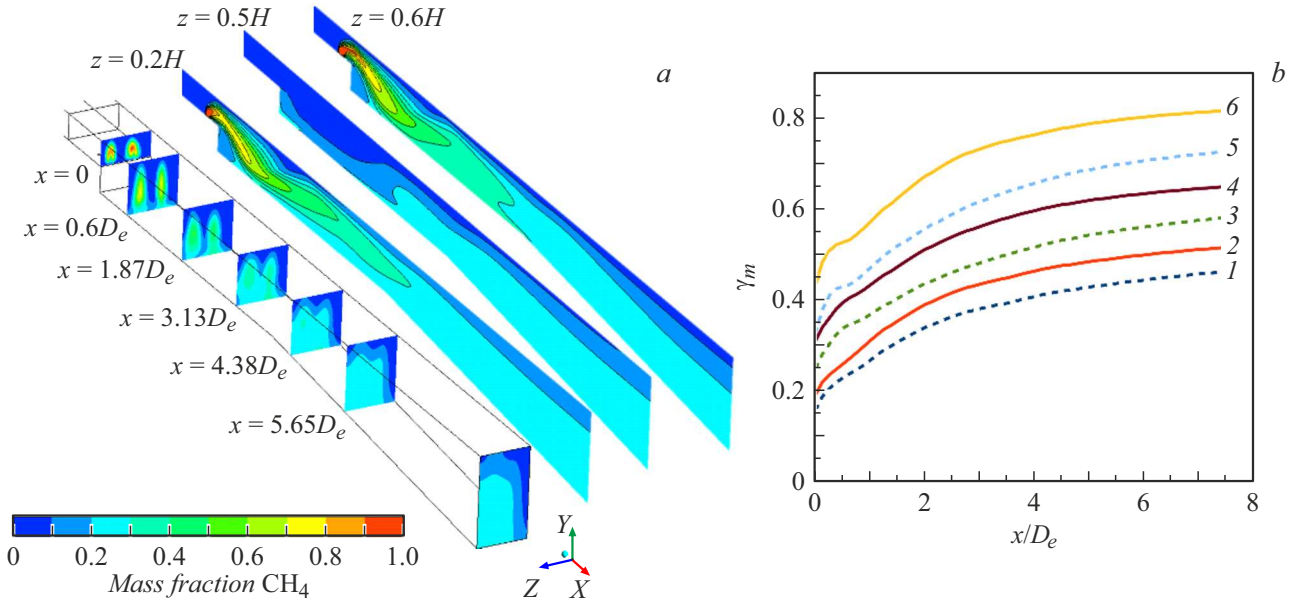


**Figure 3.** *a* — Calculated fields of the mass fraction of methane. *b* — Calculated uniformity index for hydrogen (*1*, *3*, and *5*) and methane (*2*, *4*, and *6*) at $J = 1.27$ (*1*, *2*), 3 (*3*, *4*), and 6 (*5*, *6*).

fraction of methane is minimized near the walls (especially the side one) and in the corner of the channel.

The values of mass-averaged nonuniformity index $\gamma_m$ were calculated using the formula from [9] to estimate the variation of mixing degree along the channel length. The distribution of the nonuniformity index along the channel length is presented in Fig. 3, *b*. These data indicate that the index increases at the highest rate within the channel region with a constant cross section and continues to grow more gradually in the expanding region. It should be noted that the index increases with $J$ and the values for methane are always higher than those for hydrogen at equal $J$. Notably, the difference between these values is smaller than the variation corresponding to a single-step change of the dynamic head within the examined range.

Thus, the results of calculations and experiments revealed that the injection of hydrogen and methane shifts upstream the flow pattern typical of the channel (with two peaks of static pressure). As the ratio of dynamic pressures increases, the shift magnitude and the maximum values also grow. An increase in the molecular mass induces an insignificant (relative to the width of pressure peaks) shift of maxima. The flow structure undergoes qualitative changes after the injection of hydrogen and methane. When the molecular mass increases, the mixing intensifies, and the uniformity index also grows throughout the entire channel length. The injection of gases results in enhancement of total pressure losses.

## Acknowledgments

Experiments were performed at the „Mechanics“ common use center.

## Funding

This study was carried out under the state assignment of the Khristianovich Institute of Theoretical and Applied Mechanics, Siberian Branch, Russian Academy of Sciences (state registration number 121030500162-7).

## Conflict of interest

The authors declare that they have no conflict of interest.

## References

[1] M. Sun, H. Wang, F. Xiao, *Jet in supersonic crossflow* (Springer, Singapore, 2019), p. 27–199. DOI: 10.1007/978-981-13-6025-1
[2] K.M. Pandey, T. Sivasakthivel, Int. J. Chem. Eng. Appl., **1** (4), 294 (2010). DOI: 10.7763/IJCEA.2010.V1.52
[3] W. Zhou, K. Xing, S. Dou, Q. Yang, X. Xu, Aerospace, **9** (11), 631 (2022). DOI: 10.3390/aerospace9110631
[4] A. Ben-Yakar, M.G. Mungal, R.K. Hanson, Phys. Fluids, **18** (2), 026101 (2006). DOI: 10.1063/1.2139684
[5] W. Huang, Aerospace Sci. Technol., **50**, 183 (2016). DOI: 10.1016/j.ast.2016.01.001
[6] W. Huang, J. Liu, L. Jin, L. Yan, Aerospace Sci. Technol., **32** (1), 94 (2014). DOI: 10.1016/j.ast.2013.12.006
[7] I. Rasheed, D.P. Mishra, in *Recent trends in thermal and fluid sciences*. Lecture Notes in Mechanical Engineering (Springer, 2023), p. 11–21. DOI: 10.1007/978-981-19-3498-8_2
[8] J.A. Schetz, L. Maddalena, S.K. Burger, J. Propul. Power, **26** (5), 1102 (2010). DOI: 10.2514/1.49355
[9] N.N. Fedorova, M.A. Goldfeld, Tech. Phys. Lett., **47** (1), 50 (2021). DOI: 10.1134/S1063785021010193.

[10] I. Rasheed, D.P. Mishra, in *34th National Convention of Aerospace Engineers and National Conf.* (2023). https://www.researchgate.net/publication/371633556_Effect_of_Jet_to_Freestream_Momentum_Flux_Ratio_on_Flow_Characteristics_of_a_Hydrogen_Jet_in_Supersonic_Freestream
[11] M. Gamba, M.G. Mungal, J. Fluid Mech., **780**, 226 (2015). DOI: 10.1017/jfm.2015.454
[12] A. Abdelhafez, A. Gupta, R. Balar, K. Yu, in *43rd AIAA/ASME/SAE/ASEE Joint Propulsion Conf. & Exhibit* (Cincinnati, 2007), paper AIAA 2007-5026. DOI: 10.2514/6.2007-5026
[13] A.S. Pudsey, V. Wheatley, R.R. Boyce, J. Propul. Power, **31** (1), 144 (2015). DOI: 10.2514/1.B35298
[14] M.A. Goldfeld, A.A. Maslov, A.V. Starov, V.V. Shumskii, M.I. Yaroslavtsev, AIP Conf. Proc., **1770**, 030020 (2016). DOI: 10.1063/1.4963962
[15] N.N. Fedorova, M.A. Goldfeld, S.A. Valger, J. Phys.: Conf. Ser., **1677**, 012039 (2020). DOI: 10.1088/1742-6596/1677/1/012039

*Translated by Ego Translating*